



Neurotrophic Effects of *Mu Bie Zi* (*Momordica cochinchinensis*) Seed Elucidated by High-Throughput Screening of Natural Products for NGF Mimetic Effects in PC-12 Cells

E. Mazzio¹, B. Georges², O. McTier², and Karam F. A. Soliman¹

¹ College of Pharmacy and Pharmaceutical Sciences, Florida A&M University, Room 104, Dyson Pharmacy Building, 1520 ML King, Blvd, Tallahassee, FL, 32307 USA

² Department of Biology, Florida A&M, University, Tallahassee, FL, 32307 USA

Abstract

Post-mitotic central nervous system (CNS) neurons have limited capacity for regeneration, creating a challenge in the development of effective therapeutics for spinal cord injury or neurodegenerative diseases. Furthermore, therapeutic use of human neurotrophic agents such as nerve growth factor (NGF) are limited due to hampered transport across the blood brain barrier (BBB) and a large number of peripheral side effects (e.g. neuro-inflammatory pain/tissue degeneration etc.). Therefore, there is a continued need for discovery of small molecule NGF mimetics that can penetrate the BBB and initiate CNS neuronal outgrowth/regeneration. In the current study, we conduct an exploratory high-through-put (HTP) screening of 1144 predominantly natural/herb products (947 natural herbs/plants/spices, 29 polyphenolics and 168 synthetic drugs) for ability to induce neurite outgrowth in PC12 dopaminergic cells grown on rat tail collagen, over 7 days. The data indicate a remarkably rare event-low hit ratio with only 1/1144 tested substances (<111.25 µg/mL) being capable of inducing neurite outgrowth in a dose dependent manner, identified as; *Mu Bie Zi*, *Momordica cochinchinensis* seed extract (MCS). To quantify the neurotrophic effects of MCS, 36 images (n = 6) (average of 340 cells per image), were numerically assessed for neurite length, neurite count/cell and min/max neurite length in microns (µm) using Image J software. The data show neurite elongation from 0.07 ± 0.02 µm (controls) to 5.5 ± 0.62 µm (NGF 0.5 µg/mL) and 3.39 ± 0.45 µm (138 µg/mL) in MCS, where the average maximum length per group extended from 3.58 ± 0.42 µm (controls) to 41.93 ± 3.14 µm (NGF) and 40.20 ± 2.72 µm (MCS). Imaging analysis using immunocytochemistry (ICC) confirmed that NGF and MCS had similar influence on 3-D orientation/expression of 160/200 kD neurofilament, tubulin and F-actin. These latent changes were associated with early rise in phosphorylated extracellular signal-regulated kinase (ERK) p-Erk1 (T202/Y204)/p-Erk2 (T185/Y187) at 60 min with mild changes in pAKT peaking at 5 min, and no indication of pMEK involvement. These findings demonstrate a remarkable infrequency of natural products or polyphenolic constituents to exert neurotrophic effects at low concentrations, and elucidate a unique property of MCS extract to do so. Future research will be required to delineate in depth mechanism of action of MCS, constituents responsible and potential for therapeutic application in CNS degenerative disease or injury.

Keywords

Nerve growth factor; High throughput screening; Neurotrophic; NGF mimetic; NGF signaling; Chinese herbs

Introduction

Standard treatments for neurodegenerative disorders such as Alzheimer's disease (AD), Parkinson's disease (PD), amyotrophic lateral sclerosis and Huntington's disease restore the balance of neurotransmitters enabling somewhat normal neuromotor function. While most drug regimens have capacity to improve quality of life, they do not address the underlying etiology of the disease and thereby do not arrest progression degenerative processes. Although endogenous synthesis of trophic molecules such as nerve growth factor (NGF) [1], brain-derived neurotrophic factor (BDNF) and neurotrophin-3/neurotrophin-4 can effectively stimulate neuronal growth/repair [2, 3], therapeutic applications are limited by a wide range of negative side effects such as neuropathic pain [4, 5], bladder/urinary pain [6], itchy skin (pruritus) atopical dermatitis [7 – 9], deep tissue tenderness [10, 11], exacerbated inflammatory conditions such as arthritis, asthma [10, 12, 13], inter-vertebral disc degeneration [14] and cancer [15 – 17]. Furthermore, elevated levels of NGF in various neuronal tissue can lead to behavioral/cognitive disorders such as autism [18], bipolar [19] and attention deficit/hyperactivity disorder. [20] Given the adverse systemic effects of NGF, in addition to its limited BBB transport [21, 22], oral administration is not feasible. For that reason, research focus on the use of NGF application is largely limited to its use in genetically modified mesenchymal stem cell transplants [23], biomaterial artificial 3D nerve guidance composites [24] or NGF liposomal-targeted drug delivery systems to effectively treat CNS/PNS injuries. [25, 26].

There is a seeming need for research efforts in the identification and development of small molecule NGF mimetics, which could potentially pass through the BBB and exert neurotrophic effects within the CNS, without side effect. To date, there are only a few known NGF mimetics such as GK-2 h, which in experimental models show capacity to promote neuronal survival, differentiation and synaptic plasticity demonstrating possible application for Alzheimer's disease [27], Parkinson's disease [28], cerebral ischemia [29], neural toxicity [30] or SCI [31]. The aim of the current investigation is to screen a large variety of natural plant extracts and polyphenolics, in an exploratory fashion, to elucidate substances that exert NGF mimetic effects in rat dopaminergic pheochromocytoma PC-12 cells on collagen coated plates. The findings from this study demonstrate that the aqueous extract of *Mu Bie Zi*, *Momordica cochinchinensis* seed contains inherent NGF mimetic properties, this being the only extract in the 1144 substances evaluated with this unique property.

Methods and Materials

Hanks Balanced Salt Solution (4-(2-hydroxyethyl)-1-piperazineethanesulfonic acid) (HEPES), ethanol, 96 well plates, rat tail collagen, collagen coated plates, general reagents and supplies were all purchased from Sigma-Aldrich Co. (St. Louis, MO, USA) and VWR

International (Radnor, PA, USA). Imaging probes were supplied by (Life Technologies Grand Island, NY, USA), natural products were provided by Frontier Natural Products Co-op (Norway, IA, USA), Monterey Bay Spice Company (Watsonville, CA, USA), Mountain Rose Herbs (Eugene, OR, USA), Mayway Traditional Chinese Herbs (Oakland, CA, USA), Kalyx Natural Marketplace (Camden, NY, USA), Futureceuticals (Momence, IL, USA), organic fruit vegetable markets and Florida Food Products Inc. (Eustis, FL, USA). The *Mu Bie Zi*, *M. cochinchinensis* seeds were purchased from Plum Flower Bands and Mayway Traditional Chinese Herbs (Oakland, CA, USA).

Cell Culture

PC-12 cells were obtained from ATCC (Manassas, VA, USA). Cells were cultured in high glucose DMEM [4500 mg/L glucose] containing phenol red, 5 % FBS, 4 mM L-glutamine and penicillin/streptomycin (100 U/0.1 mg/mL). The cells were maintained at 37 °C in 5 % CO₂/atmosphere. Every 2–5 days, the medium was replaced and the cells sub-cultured. For experiments, cells were disbursed into a homogenous solution of singlet cells and plated at a density of approximately 0.1×10^5 cells/mL on collagen-coated plates.

High-Throughput/Randomized: Double Bind Study

Natural products were extracted in ethanol and polyphenolics/synthetic drugs in DMSO. Subsequent dilutions were prepared in sterile HBSS (pH 7.4) so that working solutions <0.5% solvent at the highest concentrations. All cell culture flasks, dishes and 96 well plates used in this study were pre-collagen coated, or manually coated with rat-tail collagen and sterilized. For initial screening, PC-12 cells were plated in dispersed monolayers in 96 well plates, experimental treatments were added and neurite differentiation was monitored throughout a 7-day period, with in depth imaging analysis on Day 7.

Visual microscopic observation and notation of neurite outgrowth and necrotic/dead cells was established using a grid panel notation method, without knowledge of treatment—by two independent observers, and viability was later confirmed using resazurin (Alamar Blue) indicator dye [32]. A subsequent validation screen was conducted in an identical manner, where 44 noted toxic compounds were subsequently diluted 1/10 and rescreened so that 100 percent viability was confirmed in all samples. Under these conditions, evidence of neurite outgrowth was again evaluated on the seventh day, relative to NGF treated and untreated controls. Subsequently, any potential hit (defined as any observation of neurite spindle shape or neurite outgrowth however minor) was rescreened over a dose range, followed by a final validation on the single and only substance to exert potent NGF mimetic effects; *Mu Bie Zi*, *M. cochinchinensis* seed extract in a dose dependent fashion.

Cell Viability

Cell viability was determined using resazurin (Alamar Blue) indicator dye [32]. A working solution of resazurin was prepared in sterile PBS [-phenol red] (0.5 mg/mL) and added (15 % v/v) to each sample. Samples were returned to the incubator for 6–8 h and reduction of the dye by viable cells (to resorufin, a fluorescent compound) was quantitatively assessed using a microplate fluorometer, Model 7620, version 5.02 (Cambridge Technologies Inc., Watertown, MA, USA) with settings at (550 nm/580 nm), (excitation/emission).

Neurite Outgrowth

Neurite outgrowth was measured using NeuronJ—an ImageJ (IJ?1.46r) plugin enabling the tracing and quantification of elongated neurites. Briefly, 36 images were captured using an inverted microscope (25× objective phase contrast lens), n = 6. Samples consisted of PC-12 cell (–) controls, NGF treated (+) controls and cells treated with MCS from; 0.0021, 0.004, 0.0086, 0.0173, 0.0347, 0.0694, 0.1388, 0.2777, 0.5555, and 1.111 µg/mL. Cells were manually counted (average = 340 cells per image), and neurite length and count per image were quantified. Statistical analysis from numerical data provided information on average neurite length, neurite count/cell and min/max neurite extension length in microns (µm).

Immunocytochemistry and Fluorescence Microscopy

Cells were fixed in 4 % paraformaldehyde for 15 min, and subsequently permeabilized in 0.25 % triton X-100 prepared in phosphate buffered saline (PBS) for 15 min. Briefly, stock solutions containing fluorescent probes were prepared by dissolving 5 mg/1 mL ethanol, then subsequently diluted in HBSS and added to cells : final dye concentration—5 µg/mL propidium iodide (PI) and 6.6 µM (phalloidin). Photographic images reflect Alexa Fluor[®] 488 phalloidin/PI nuclear counter stain and tubulin which were acquired using a TubulinTracker[™] Oregon Green[®] 488 Taxol, bis-acetate probe (Life Technologies Inc.). Cytoskeletal changes were captured using live morphological imaging and immunocytochemistry on fixed permeabilized cells—using primary rabbit anti-rat neurofilament 160/200 and 200 antibodies, conjugated to goat anti-rabbit Alexa Fluor[®] 488. Samples were analyzed photographically using an fluorescent/inverted microscope, CCD camera and data acquisition using ToupTek View (TouTek Photonics Co, Zhejiang, People's Republic of China).

NGF Signaling

Signaling was evaluated using sandwich ELISA kits to assay for quantification of Akt (pS473) + total Akt, Erk1 (pT202/pY204) + Erk2 (pT185/pY187) + total Erk1/2 and Mek1 (pS217/221) + total Mek1. Reagents were purchased from Abcam (Cambridge, MA, USA) and manufacturers protocols were adhered to. Briefly, cells were placed in lysate buffer with protease and phosphatase inhibitors and placed on ice for 30 min. Samples were frozen at—80 °C, subject to two rapid freeze thaw cycles and centrifuged. In brief, cells were treated with various concentrations of NGF, or MCS for 15 min to 7 days in order to establish approximate time dependent signaling effects. The largest shift occurred in the phosphorylation of ERK around 60 min. Subsequent signaling studies were conducted (n = 4) between 0 and 60 min, where media was removed from the wells; cells were lysed and transferred to replicate wells of the ELISA kits. After linking from 2.5 h to overnight at 4 °C, wells were washed and incubated with 1° antibody, follows by a wash and a 2° secondary HRP-conjugated anti-body followed by a final wash which preceded a colorimetric reaction initiated by addition of a TMB substrate solution. After 30 min, a stop solution was added and O.D. measured at 450 nm microplate reader (BioTek Instruments, Inc., Wincoski, VT, USA).

Data Analysis

Statistical analysis was performed using Graph Pad Prism (version 3.0; Graph Pad Software Inc. San Diego, CA, USA) with significance of difference between the groups assessed using a one-way ANOVA, followed by Tukey post hoc means comparison test. IC₅₀s were determined by regression analysis using Origin Software (OriginLab, Northampton, MA, USA).

Results

A high through put screening of 1144 compounds: 29 plant based polyphenolics (11.12 µg/mL), 168 synthetic/control drugs (including celcoxib, ibuprofen, paclitaxel etc.) (1.112 µg/mL) and extracts of 947 commonly used herbs and spices (111.25 µg/mL) were evaluated for ability to induce neurite extension in PC-12 cells relative to a NGF control on collagen coated plates (Fig. 1 a). The initial screen was conducted twice, using double blind microscopic observations by two individuals. Toxicity was established for 44 compounds, to which the entire screening was repeated, with dilution of these (44) toxic compounds 1:10. A repeat screening for neurotrophic effects of all compounds was conducted, where no toxicity was observed for any experimental treatment [confirmed by Alamar blue (data not shown)]. Lastly, 77 compounds were retested (based on any slight evidence of neurite outgrowth) over a dose response of six concentrations (1– 500 µg/mL). Of these, there was one positive hit—which caused dose dependent neurite outgrowth. While many of the compounds showed insignificant or meager neurite outgrowth—none of these were dose responsive, except for the MCS *Mu Bie Zi*, *M. cochinchinensis* seed extract (Fig. 1 b).

To establish quantitative neurite outgrowth by MCS versus NGF, 36 images were acquired and quantification parameters included total cell count/frame; total neurite count/frame; total neurite length/frame; average neurite length/frame; neurite count/cell; neurite length/cell and min and max neurite length. Groups were classified as MCS extract treated (4–138 µg/mL), negative control (–NGF) and positive control (NGF 0.5 µg/mL) (Table 1). The data show that MCS induced neurite length from an average of 0.07 ± 0.02 microns (control) to 5.5 ± 0.62 microns (NGF 0.5 µg/mL) and 3.39 ± 0.45 microns (138 µg/mL) in MCS (Fig. 2 a). Also evident, were the changes in maximum neurite length (Fig. 2 b) and neurite extension per cell by NGF and MCS (Fig. 2 c). The effects of MCS and NGF were similar in that neurite outgrowth was also associated with cell differentiation, elongated extension and halt of mitosis—corroborated by gradual reduction in cell count per frame.

Morphological imaging also showed extensive NGF and MCS neurite development (Fig. 1 b), with major changes in structure, organization and concentration of neurofilament of 200 kD (Fig. 3 a), F-actin, combined 160/120 kD neurofilaments (Fig. 3 b) and tubulin (Fig. 3 c). A pilot test evaluating early signaling events associated with NGF and MCS included ERK phosphorylation at 60 min (Fig. 4 a), with no effects on MEK/MEK-p (Fig. 4 b) and meager phosphorylation of AKT at 5 min after NGF/MCS was added to the cells (Fig. 4 c). These findings identify a novel and unique natural compound with NGF mimetic effects, albeit the mechanism of action and constituents within need further elucidation.

Discussion

The neuro-protective/ trophic properties of NGF are well established [24, 30, 31], albeit therapeutic applications are currently limited due to pathogenic side effects including neuropathic [4, 5] and deep tissue pain [10, 11] atopic dermatitis [7 – 9], arthritis, asthma [10, 12, 13], intervertebral disc degeneration [14] and cancer. [15 – 17] Therefore, there is a need for identification of small MW neurotrophic compounds that may have therapeutic value in treatment of peripheral/CNS injury or neurodegenerative disorders, without the limitations of endogenous neurotrophins. The findings from this study indicate the infrequency of natural plant based extracts or substances to induce neurite outgrowth in the PC-12 cell model, to the exception of unique extracts such as that of *M. cochinchinensis* seed (MCS).

The capacity of MCS to induce neurite outgrowth in PC-12 cells is less extensive than NGF, but demonstrates a similarity in change of structural proteins such as actin, tubulin and neurofilaments as demonstrated within. Both NGF and MCS can induce morphological changes NF200, which plays a critical role in preventing axonal neuron degeneration after brain [33], or spinal cord injury [34] and used to efficacy of neurological therapies [35, 36]. NGF signaling by a mimetic is likely to induce cellular reorganization/elongation of cytoskeletal microtubules (formation of neuritic shafts) and development of filopodia/ lamellipodia with flexible growth cones that extend along a biological matrix (e.g. collagen). [37 – 39] Internal signaling associated with these outward manifestations, include phosphorylation of tropomyosin-related kinase receptor (Trk) (A–C), the subsequent early rise in pERK (1/2)/cAMP signaling, late phase endosomal internalization of the TrKA receptor complex [40 – 43] and stimulation of microtubule binding proteins which act on tubulin polymers, F-actin microfilaments and G-actin tetramers. [44, 45] The data from this study suggest that neither NGF or MCS extract had an effect on pMEK, only a slight early (5 min) elevation of pAKT with pronounced effects on pERK1/2 at about 60 min. Likewise, research throughout the literature is fairly consistent reporting the NGF invoked rise in pERK1/2 [46 – 49] and pAKT [47 – 49] as well as cAMP [50, 51], protein kinase A, pCREB [46 – 49] with inconsistent reports for p38MAPK. [49] Future research will be required to evaluate these signaling pathways in the presence of MCS.

While rapid early signaling events control the initial impact of NGF, clearly neurite outgrowth is a lengthy process in PC-12 cells—occurring over a 3– 7 days period. It is believed that long term signaling effects involve NGF-TrkA endocytosis into endosomes with Rab22GTPase [40 – 43, 52] and a stabilizing protein such as coronin-1 [53], which can then initiate restructure of the membrane cytoskeleton in conjunction Rho GTPase Rac1, cdc42 and Tc10. [54, 55] These processes, while not investigated in the current study, are believed to be integral to initial formations of lamellipodia, filopodia or stress fibers. [37 – 39], which are subject to retraction and polymerizing of F-actin involved with neurite outgrowth [44, 45]. In addition, there are hundreds of actin binding proteins (ABPs) that assist in this process, with specific roles in F-actin crosslinking, severing, polymerization (growth), retraction and end capping at the growth cones. ABP concentrations highly abundant in growth cones consists of Arp2/3, ccdc8, cortactin, GAP-43 or syntaxin 6 [56] responsible for neurite extension elongation [31, 57]. Other wide type extensions often

observed in NGF-treated PC12 cells termed “varicones” are concentrated in proteins such as synaptophysin, calpain2, syntaxin. [58].

Although, future research will be required on MCS extract, we do know that the seeds are orange/red in color due to lycopene [59, 60] and it has significant concentrations of triterpenoidal saponins, gypsogenin and quillaic acid glycosides [61] and low MW cell penetrating dipeptides [62] such as cochinin B (28 kDa) [63] and *M. cochinchinensis* trypsin inhibitor I (MCoTI-I) and 2 (MCoTI-II). [64] MCoTI-II belongs to the cyclotide family of plant-derived cyclic peptides that are characterized by a cyclic cystine knot motif [65, 66] known to be thermally and chemically stable, and resistant to enzymatic degradation. [67, 68] MCS derived cyclic knottins share similar conformational form as noncyclic squash inhibitors such as CPTI [69] and interesting also, NGF [70]. While NGF medicinal applications are limited, natural NGF mimetics such as those found in the MCS extract are generally robust in therapeutic properties previously reported to have anti-viral, [71, 72] anti-angiogenic, anti-tumor [73] anti-inflammatory and anti-oxidant properties [63] and an ability to enhance innate immunity [74, 75], aid in wound healing [76] and heal gastric ulcers. [77].

Conclusions

In summary, these findings suggest that aqueous extract of *M. cochinchinensis* seeds exert NGF mimetic effects, through early pERK signaling and morphological changes in structural proteins associated with neurite branching and outgrowth. Future research will be required to evaluate if known small MW peptides containing a similar cystine knot motif to that of NGF, are responsible for these effects and if so—further developments could lead to a therapeutic drug application of NGF mimetics within to enhance recovery of peripheral and central nervous system injuries.

Acknowledgments

This project was supported by the National Institutes of Health, National Institute of Minority Health and Health Disparities, RCMI Grant (8G12MD007582-28.) and COE Grant (P20 MD006738).

References

1. Levi-Montalcini R, Cohen S. In vitro and in vivo effects of a nerve growth-stimulating agent isolated from snake venom. Proc Natl Acad Sci USA. 1956; 42:695–699. [PubMed: 16589933]
2. Esmaeili A, Alifarja S, Nourbakhsh N, Talebi A. Messenger RNA expression patterns of neurotrophins during transdifferentiation of stem cells from human-exfoliated deciduous teeth into neural-like cells. Avicenna J Med Biotechnol. 2014; 6:21–26. [PubMed: 24551431]
3. Bothwell M. NGF, BDNF, NT3, and NT4. Handb Exp Pharmacol. 2014; 220:3–15. [PubMed: 24668467]
4. Pezet S. Neurotrophins and pain. Biol Aujourd'hui. 2014; 208:21–29. [PubMed: 24948016]
5. Muralidharan A, Wyse BD, Smith MT. Analgesic efficacy and mode of action of a selective small molecule angiotensin II type 2 receptor antagonist in a rat model of prostate cancer-induced bone pain. Pain Med. 2014; 15:93–110. [PubMed: 24433468]
6. Kim SW, Im YJ, Choi HC, Kang HJ, Kim JY, Kim JH. Urinary nerve growth factor correlates with the severity of urgency and pain. Int Urogynecol J. 2014; 25:1561–1567. [PubMed: 24866276]

7. Ono R, Kagawa Y, Takahashi Y, Akagi M, Kamei C. Effect of 2,3,7,8-tetrachlorodibenzo-p-dioxin on scratching behavior in mice. *Int Immunopharmacol.* 2010; 10:304–307. [PubMed: 19969104]
8. Yosipovitch G. Dry skin and impairment of barrier function associated with itch—new insights. *Int J Cosmet Sci.* 2004; 26:1–7. [PubMed: 18494919]
9. Teresiak-Mikolajczak E, Czarnecka-Operacz M, Jenerowicz D, Silny W. Neurogenic markers of the inflammatory process in atopic dermatitis: relation to the severity and pruritus. *Postepy Dermatologii i Alergologii.* 2013; 30:286–292. [PubMed: 24353488]
10. McMahon SB, Cafferty WB, Marchand F. Immune and glial cell factors as pain mediators and modulators. *Exp Neurol.* 2005; 192:444–462. [PubMed: 15755561]
11. Bannwarth B, Kostine M. Targeting nerve growth factor (NGF) for pain management: what does the future hold for NGF antagonists? *Drugs.* 2014; 74:619–626. [PubMed: 24691709]
12. Kim JS, Kang JY, Ha JH, Lee HY, Kim SJ, Kim SC, Ahn JH, Kwon SS, Kim YK, Lee SY. Expression of nerve growth factor and matrix metalloproteinase-9/tissue inhibitor of metalloproteinase-1 in asthmatic patients. *J Asthma: Off J Assoc Care Asthma.* 2013; 50:712–717.
13. Chen YL, Huang HY, Lee CC, Chiang BL. Small interfering RNA targeting nerve growth factor alleviates allergic airway hyperresponsiveness. *Mol Ther Nucleic Acids.* 2014; 3:e158. [PubMed: 24714423]
14. Kao TH, Peng YJ, Tsou HK, Salter DM, Lee HS. Nerve growth factor promotes expression of novel genes in intervertebral disc cells that regulate tissue degradation. *J Neurosurg Spine* 1–9Spine. 2014; 21:653–656.
15. Vinoses SA, Perez-Polo JR. Nerve growth factor and neural oncology. *J Neurosci Res.* 1983; 9:81–100. [PubMed: 6300414]
16. Wang W, Chen J, Guo X. The role of nerve growth factor and its receptors in tumorigenesis and cancer pain. *Biosci Trends.* 2014; 8:68–74. [PubMed: 24815383]
17. Hondermarck H. Neurotrophins and their receptors in breast cancer. *Cytokine Growth Factor Rev.* 2012; 23:357–365. [PubMed: 22749855]
18. Dincel N, Unalp A, Kutlu A, Ozturk A, Uran N, Ulusoy S. Serum nerve growth factor levels in autistic children in Turkish population: a preliminary study. *Indian J Med Res.* 2013; 138:900–903. [PubMed: 24521633]
19. Barbosa IG, Huguet RB, Neves FS, Reis HJ, Bauer ME, Janka Z, Palotas A, Teixeira AL. Impaired nerve growth factor homeostasis in patients with bipolar disorder. *World J Biol Psychiatry.* 2011; 12:228–232. [PubMed: 20923384]
20. Guney E, Ceylan MF, Kara M, Tekin N, Goker Z, Senses Dinc G, Ozturk O, Eker S, Kizilgun M. Serum nerve growth factor (NGF) levels in children with attention deficit/hyperactivity disorder (ADHD). *Neurosci Lett.* 2014; 560:107–111. [PubMed: 24361544]
21. Backman C, Rose GM, Hoffer BJ, Henry MA, Bartus RT, Friden P, Granholm AC. Systemic administration of a nerve growth factor conjugate reverses age-related cognitive dysfunction and prevents cholinergic neuron atrophy. *J Neurosci.* 1996; 16:5437–5442. [PubMed: 8757256]
22. Poduslo JF, Curran GL. Permeability at the blood–brain and blood–nerve barriers of the neurotrophic factors: NGF, CNTF, NT-3, BDNF. *Brain Res Mol Brain Res.* 1996; 36:280–286. [PubMed: 8965648]
23. Cui X, Chen L, Ren Y, Ji Y, Liu W, Liu J, Yan Q, Cheng L, Sun YE. Genetic modification of mesenchymal stem cells in spinal cord injury repair strategies. *Biosci Trends.* 2013; 7:202–208. [PubMed: 24241170]
24. Kuihua Z, Chunyang W, Cunyi F, Xiumei M. Aligned SF/P(LLA-CL)-blended nanofibers encapsulating nerve growth factor for peripheral nerve regeneration. *J Biomed Mater Res, Part A.* 2014; 102:2680–2691.
25. Kuo YC, Wang CT. Protection of SK-N-MC cells against beta-amyloid peptide-induced degeneration using neuron growth factor-loaded liposomes with surface lactoferrin. *Biomaterials.* 2014; 35:5954–5964. [PubMed: 24746790]
26. Yu H, Liu J, Ma J, Xiang L. Local delivery of controlled released nerve growth factor promotes sciatic nerve regeneration after crush injury. *Neurosci Lett.* 2014; 566:177–181. [PubMed: 24614335]

27. Povarnina PY, Vorontsova ON, Gudasheva TA, Ostrovskaya RU, Seredenin SB. Original nerve growth factor mimetic dipeptide GK-2 restores impaired cognitive functions in rat models of Alzheimer's disease. *Acta Naturae*. 2013; 5:84–91. [PubMed: 24303204]
28. Antipova TA, Gudasheva TA, Seredenin SB. In vitro study of neuroprotective properties of GK-2, a new original nerve growth factor mimetic. *Bull Exp Biol Med*. 2011; 150:607–609. [PubMed: 22235396]
29. Povarina P, Gudasheva TA, Vorontsova ON, Nikolaev SV, Antipova TA, Ostrovskaya RU, Seredin SB. Neuroprotective effects of a dipeptide mimetic on the GK-2 nerve growth factor in model of permanent common carotid artery occlusion in rats. *Eksperimental'naiia i Klinicheskaia Farmakologiya*. 2012; 75:15–20.
30. Zhao GY, Ding XD, Guo Y, Chen WM. Intrathecal lidocaine neurotoxicity: combination with bupivacaine and ropivacaine and effect of nerve growth factor. *Life Sci*. 2014; 112:10–21. [PubMed: 25064827]
31. Zhang H, Wu F, Kong X, Yang J, Chen H, Deng L, Cheng Y, Ye L, Zhu S, Zhang X, Wang Z, Shi H, Fu X, Li X, Xu H, Lin L, Xiao J. Nerve growth factor improves functional recovery by inhibiting endoplasmic reticulum stress-induced neuronal apoptosis in rats with spinal cord injury. *J Transl Med*. 2014; 12:130. [PubMed: 24884850]
32. Evans SM, Casartelli A, Herreros E, Minnick DT, Day C, George E, Westmoreland C. Development of a high throughput in vitro toxicity screen predictive of high acute in vivo toxic potential. *Toxicol In Vitro*. 2001; 15:579–584. [PubMed: 11566594]
33. Dileonardi AM, Huh JW, Raghupathi R. Differential effects of FK506 on structural and functional axonal deficits after diffuse brain injury in the immature rat. *J Neuropathol Exp Neurol*. 2012; 71:959–972. [PubMed: 23095847]
34. Cheng L, Liu Y, Zhao H, Zhang W, Guo YJ, Nie L. Lentiviral-mediated transfer of CDNF promotes nerve regeneration and functional recovery after sciatic nerve injury in adult rats. *Biochem Biophys Res Commun*. 2013; 440:330–335. [PubMed: 24076387]
35. Figley SA, Liu Y, Karadimas SK, Satkunendrarajah K, Fettes P, Spratt SK, Lee G, Ando D, Surosky R, Giedlin M, Fehlings MG. Delayed administration of a bio-engineered zinc-finger VEGF-A gene therapy is neuroprotective and attenuates allodynia following traumatic spinal cord injury. *PLoS One*. 2014; 9:e96137. [PubMed: 24846143]
36. Chen G, Zhang Z, Wang S, Lv D. Combined treatment with FK506 and nerve growth factor for spinal cord injury in rats. *Exp Ther Med*. 2013; 6:868–872. [PubMed: 24137280]
37. Nuttall RP, Zinsmeister PP. Differential response to contact during embryonic nerve–nonnerve cell interactions. *Cell Motil*. 1983; 3:307–320. [PubMed: 6640630]
38. Aletta JM, Greene LA. Growth cone configuration and advance: a time-lapse study using video-enhanced differential interference contrast microscopy. *J Neurosci*. 1988; 8:1425–1435. [PubMed: 3282037]
39. Robbins N, Polak J. Filopodia, lamellipodia and retractions at mouse neuromuscular junctions. *J Neurocytol*. 1988; 17:545–561. [PubMed: 3142968]
40. Mitchell DJ, Blasier KR, Jeffery ED, Ross MW, Pullikuth AK, Suo D, Park J, Smiley WR, Lo KW, Shabanowitz J, Deppmann CD, Trinidad JC, Hunt DF, Catling AD, Pfister KK. Trk activation of the ERK1/2 kinase pathway stimulates intermediate chain phosphorylation and recruits cytoplasmic dynein to signaling endosomes for retrograde axonal transport. *J Neurosci*. 2012; 32:15495–15510. [PubMed: 23115187]
41. Song EJ, Yoo YS. Nerve growth factor-induced neurite outgrowth is potentiated by stabilization of TrkA receptors. *BMB Rep*. 2011; 44:182–186. [PubMed: 21429296]
42. Abu El-Asrar AM, Mohammad G, De Hertogh G, Nawaz MI, Van Den Eynde K, Siddiquei MM, Struyf S, Opdenakker G, Geboes K. Neurotrophins and neurotrophin receptors in proliferative diabetic retinopathy. *PLoS One*. 2013; 8:e65472. [PubMed: 23762379]
43. Arimura N, Kimura T, Nakamura S, Taya S, Funahashi Y, Hattori A, Shimada A, Menager C, Kawabata S, Fujii K, Iwamatsu A, Segal RA, Fukuda M, Kaibuchi K. Anterograde transport of TrkB in axons is mediated by direct interaction with Slp1 and Rab27. *Dev Cell*. 2009; 16:675–686. [PubMed: 19460344]

44. Pradines A, Magazin M, Schiltz P, Le Fur G, Caput D, Ferrara P. Evidence for nerve growth factor-potentiating activities of the nonpeptidic compound SR 57746A in PC12 cells. *J Neurochem.* 1995; 64:1954–1964. [PubMed: 7722483]
45. Nielander HB, French P, Oestreicher AB, Gispen WH, Schotman P. Spontaneous morphological changes by overexpression of the growth-associated protein B-50/GAP-43 in a PC12 cell line. *Neurosci Lett.* 1993; 162:46–50. [PubMed: 8121634]
46. Thauerer B, Voegelé P, Hermann-Kleiter N, Thuille N, de Araujo ME, Offterdinger M, Baier G, Huber LA, Baier-Bitterlich G. LAMTOR2-mediated modulation of NGF/MAPK activation kinetics during differentiation of PC12 cells. *PLoS One.* 2014; 9:e95863. [PubMed: 24752675]
47. Chen JH, Lee DC, Chiu IM. Cytotoxic effects of acrylamide in nerve growth factor or fibroblast growth factor 1-induced neurite outgrowth in PC12 cells. *Arch Toxicol.* 2014; 88:769–780. [PubMed: 24318646]
48. Terada K, Kojima Y, Watanabe T, Izumo N, Chiba K, Karube Y. Inhibition of nerve growth factor-induced neurite outgrowth from PC12 cells by dexamethasone: signaling pathways through the glucocorticoid receptor and phosphorylated Akt and ERK1/2. *PLoS One.* 2014; 9:e93223. [PubMed: 24667984]
49. Nishina A, Kimura H, Tsukagoshi H, Kozawa K, Koketsu M, Ninomiya M, Sato D, Obara Y, Furukawa S. Neurite outgrowth of PC12 cells by 4'-O-beta-D-glucopyranosyl-3',4'-dimethoxychalcone from *Brassica rapa L. 'hidabeni'* was enhanced by pretreatment with p38MAPK inhibitor. *Neurochem Res.* 2013; 38:2397–2407. [PubMed: 24057400]
50. Chijiwa T, Mishima A, Hagiwara M, Sano M, Hayashi K, Inoue T, Naito K, Toshioka T, Hidaka H. Inhibition of forskolin-induced neurite outgrowth and protein phosphorylation by a newly synthesized selective inhibitor of cyclic AMP-dependent protein kinase, N-[2-(p-bromocinnamylamino)ethyl]-5-isoquinolinesulfonamide (H-89), of PC12D pheochromocytoma cells. *J Biol Chem.* 1990; 265:5267–5272. [PubMed: 2156866]
51. Emery AC, Eiden MV, Eiden LE. Separate cyclic AMP sensors for neuritogenesis, growth arrest, and survival of neuroendocrine cells. *J Biol Chem.* 2014; 289:10126–10139. [PubMed: 24567337]
52. Wang L, Liang Z, Li G. Rab22 controls NGF signaling and neurite outgrowth in PC12 cells. *Mol Biol Cell.* 2011; 22:3853–3860. [PubMed: 21849477]
53. Suo D, Park J, Harrington AW, Zweifel LS, Mihalas S, Deppmann CD. Coronin-1 is a neurotrophin endosomal effector that is required for developmental competition for survival. *Nat Neurosci.* 2014; 17:36–45. [PubMed: 24270184]
54. Fujita A, Koinuma S, Yasuda S, Nagai H, Kamiguchi H, Wada N, Nakamura T. GTP hydrolysis of TC10 promotes neurite outgrowth through exocytic fusion of Rab11- and L1-containing vesicles by releasing exocyst component Exo70. *PLoS One.* 2013; 8:e79689. [PubMed: 24223996]
55. Pommereit D, Wouters FS. An NGF-induced Exo70-TC10 complex locally antagonises Cdc42-mediated activation of N-WASP to modulate neurite outgrowth. *J Cell Sci.* 2007; 120:2694–2705. [PubMed: 17635999]
56. Kabayama H, Tokushige N, Takeuchi M, Mikoshiba K. Syntaxin 6 regulates nerve growth factor-dependent neurite outgrowth. *Neurosci Lett.* 2008; 436:340–344. [PubMed: 18406529]
57. Spillane M, Ketschek A, Donnelly CJ, Pacheco A, Twiss JL, Gallo G. Nerve growth factor-induced formation of axonal filopodia and collateral branches involves the intra-axonal synthesis of regulators of the actin-nucleating Arp2/3 complex. *J Neurosci.* 2012; 32:17671–17689. [PubMed: 23223289]
58. Mingorance-Le Meur A, Mohebiany AN, O'Connor TP. Varicones and growth cones: two neurite terminals in PC12 cells. *PLoS One.* 2009; 4:e4334. [PubMed: 19183810]
59. Phan-Thi H, Wache Y. Isomerization and increase in the antioxidant properties of lycopene from *Momordica cochinchinensis* (gac) by moderate heat treatment with UV-Vis spectra as a marker. *Food Chem.* 2014; 156:58–63. [PubMed: 24629938]
60. Aoki H, Kieu NT, Kuze N, Tomisaka K, Van Chuyen N. Carotenoid pigments in GAC fruit (*Momordica cochinchinensis* SPRENG). *Biosci Biotechnol Biochem.* 2002; 66:2479–2482. [PubMed: 12506992]

61. Jung K, Chin YW, Yoon K, Chae HS, Kim CY, Yoo H, Kim J. Anti-inflammatory properties of a triterpenoidal glycoside from *Momordica cochinchinensis* in LPS-stimulated macrophages. *Immunopharmacol Immunotoxicol*. 2013; 35:8–14. [PubMed: 22916793]
62. Ng TB, Chan WY, Yeung HW. Proteins with abortifacient, ribosome inactivating, immunomodulatory, antitumor and anti-AIDS activities from Cucurbitaceae plants. *Gen Pharmacol*. 1992; 23:579–590. [PubMed: 1397965]
63. Wong KL, Wong RN, Zhang L, Liu WK, Ng TB, Shaw PC, Kwok PC, Lai YM, Zhang ZJ, Zhang Y, Tong Y, Cheung HP, Lu J, Sze SC. Bioactive proteins and peptides isolated from Chinese medicines with pharmaceutical potential. *Chin Med*. 2014; 9:19. [PubMed: 25067942]
64. D'Souza C, Henriques ST, Wang CK, Craik DJ. Structural parameters modulating the cellular uptake of disulfide-rich cyclic cell-penetrating peptides: MCoTI-II and SFTI-1. *Eur J Med Chem*. 2014; 88:10–18. [PubMed: 24985034]
65. Cascales L, Henriques ST, Kerr MC, Huang YH, Sweet MJ, Daly NL, Craik DJ. Identification and characterization of a new family of cell-penetrating peptides: cyclic cell-penetrating peptides. *J Biol Chem*. 2011; 286:36932–36943. [PubMed: 21873420]
66. Chan LY, He W, Tan N, Zeng G, Craik DJ, Daly NL. A new family of cystine knot peptides from the seeds of *Momordica cochinchinensis*. *Peptides*. 2013; 39:29–35. [PubMed: 23127518]
67. Craik DJ, Simonsen S, Daly NL. The cyclotides: novel macrocyclic peptides as scaffolds in drug design. *Curr Opin Drug Discov Dev*. 2002; 5:251–260.
68. Park S, Stromstedt AA, Goransson U. Cyclotide structure-activity relationships: qualitative and quantitative approaches linking cytotoxic and anthelmintic activity to the clustering of physicochemical forces. *PLoS One*. 2014; 9:e91430. [PubMed: 24682019]
69. Heitz A, Hernandez JF, Gagnon J, Hong TT, Pham TT, Nguyen TM, Le-Nguyen D, Chiche L. Solution structure of the squash trypsin inhibitor MCoTI-II. A new family for cyclic knottins. *Biochemistry*. 2001; 40:7973–7983. [PubMed: 11434766]
70. Kliemann M, Weininger U, Balbach J, Schwarz E, Rudolph R. Examination of the slow unfolding of pro-nerve growth factor argues against a loop threading mechanism for nerve growth factor. *Biochemistry*. 2006; 45:3517–3524. [PubMed: 16533032]
71. Oyuntsetseg N, Khasnatinov MA, Molor-Erdene P, Oyunbileg J, Liapunov AV, Danchinova GA, Oldokh S, Baigalmaa J, Chimedraghaa C. Evaluation of direct antiviral activity of the Deva-5 herb formulation and extracts of five Asian plants against influenza A virus H3N8. *BMC Complement Altern Med*. 2014; 14:235. [PubMed: 25012588]
72. Thongyoo P, Roque-Rosell N, Leatherbarrow RJ, Tate EW. Chemical and biomimetic total syntheses of natural and engineered MCoTI cyclotides. *Org Biomol Chem*. 2008; 6:1462–1470. [PubMed: 18385853]
73. Zheng L, Zhang YM, Zhan YZ, Liu CX. *Momordica cochinchinensis* seed extracts suppress migration and invasion of human breast cancer ZR-75-30 cells via down-regulating MMP-2 and MMP-9. *Asian Pac J Cancer Prev*. 2014; 15:1105–1110. [PubMed: 24606426]
74. Rajput ZI, Xiao CW, Hu SH, Habib M, Soomro NA. Enhancement of immune responses to infectious bursal disease vaccine by supplement of an extract made from *Momordica cochinchinensis* (Lour.). Spreng. seeds. *Poult Sci*. 2010; 89:1129–1135. [PubMed: 20460658]
75. Tsoi AY, Ng TB, Fong WP. Immunomodulatory activity of a chymotrypsin inhibitor from *Momordica cochinchinensis* seeds. *J Pept Sci*. 2006; 12:605–611. [PubMed: 16733830]
76. Jung K, Chin YW, Chung YH, Park YH, Yoo H, Min DS, Lee B, Kim J. Anti-gastritis and wound healing effects of Momordicaceae Semen extract and its active component. *Immunopharmacol Immunotoxicol*. 2013; 35:126–132. [PubMed: 22889079]
77. Kang JM, Kim N, Kim B, Kim JH, Lee BY, Park JH, Lee MK, Lee HS, Kim JS, Jung HC, Song IS. Enhancement of gastric ulcer healing and angiogenesis by cochinchina *Momordica* seed extract in rats. *J Korean Med Sci*. 2010; 25:875–881. [PubMed: 20514308]

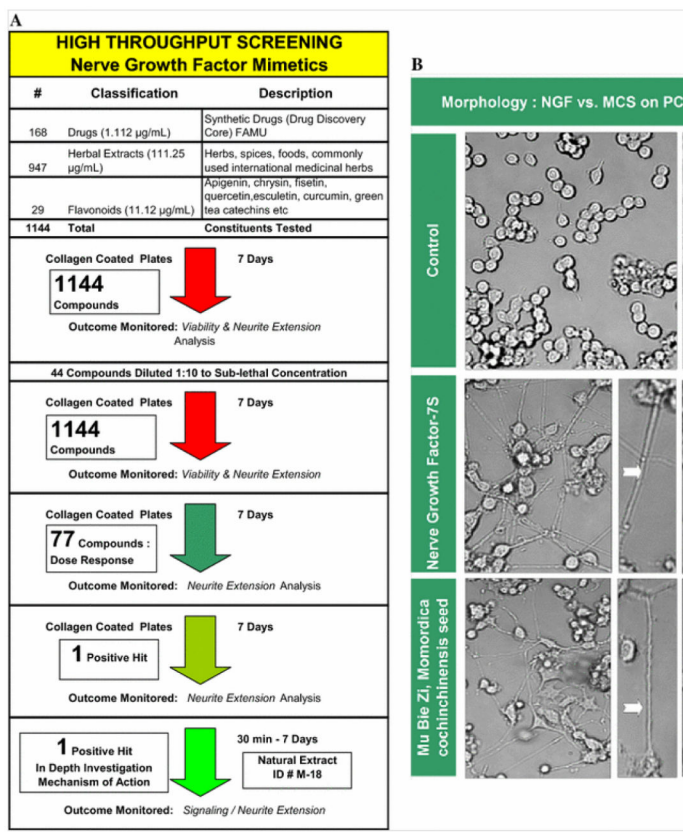
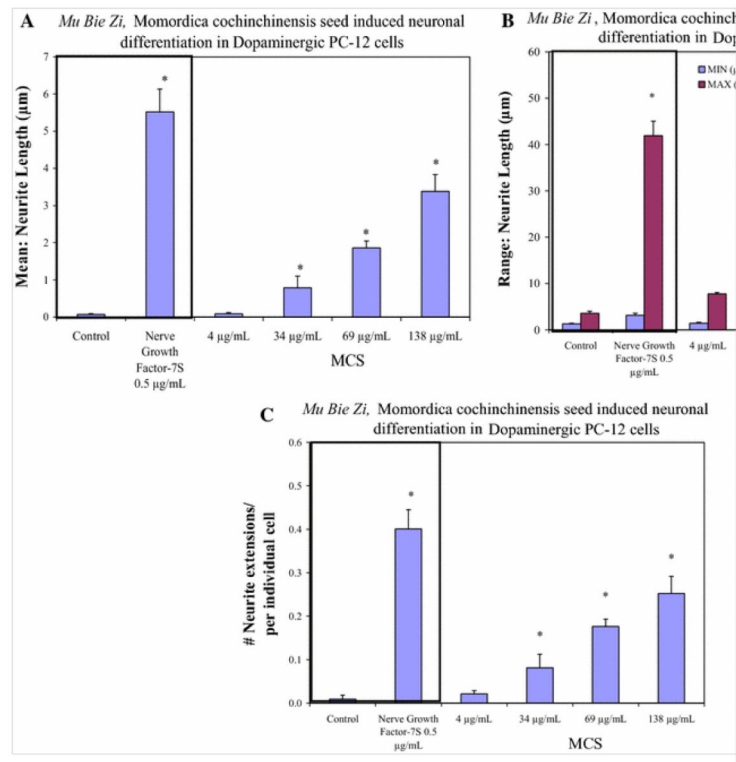


Fig. 1. **a** High throughput screening layout of 1144 plant based polyphenolics, synthetic/control drugs (including celcoxib, ibuprofen, paclitaxel etc.) and aqueous extracts of 947 commonly used herbs and spices for ability to induce neurite outgrowth in PC-12 cells relative to NGF on collagen coated plates over 7 days. Of the initial screened, with subsequent validation using a full dose range, only one positive NGF mimetic was elucidated. **b** Morphological analysis of neurite outgrowth in PC12 cells at 7 days; controls (*top*) NGF 0.5 µg/mL (*mid*) and MCS extract (150 µg/mL) (*bottom*)

**Fig. 2.**

a Effects of MCS relative to NGF on neurite extension length in PC12 cells at 7 days. The data represent average neurite length (microns) and are expressed as the mean \pm SEM, $n = 6$ images. Significant differences from the control were evaluated using a one-way ANOVA, with a Tukey post hoc test, $*P < 0.05$. **b** Effects of MCS relative to NGF on neurite minimum and maximum neurite length in PC12 cells at 7 days. The data represent average Min. or Max. (microns) and are expressed as the mean \pm SEM, $n = 6$ images. Significant differences from the control were evaluated using a one-way ANOVA, with a Tukey post hoc test, $*P < 0.05$. **c** Effects of MCS relative to NGF on neurite outgrowth in PC12 cells at 7 days. The data represent average # neurites/# cells per image—and are expressed as the mean \pm SEM, $n = 6$ images. Significant differences from the control were evaluated using a one-way ANOVA, with a Tukey post hoc test, $*P < 0.05$

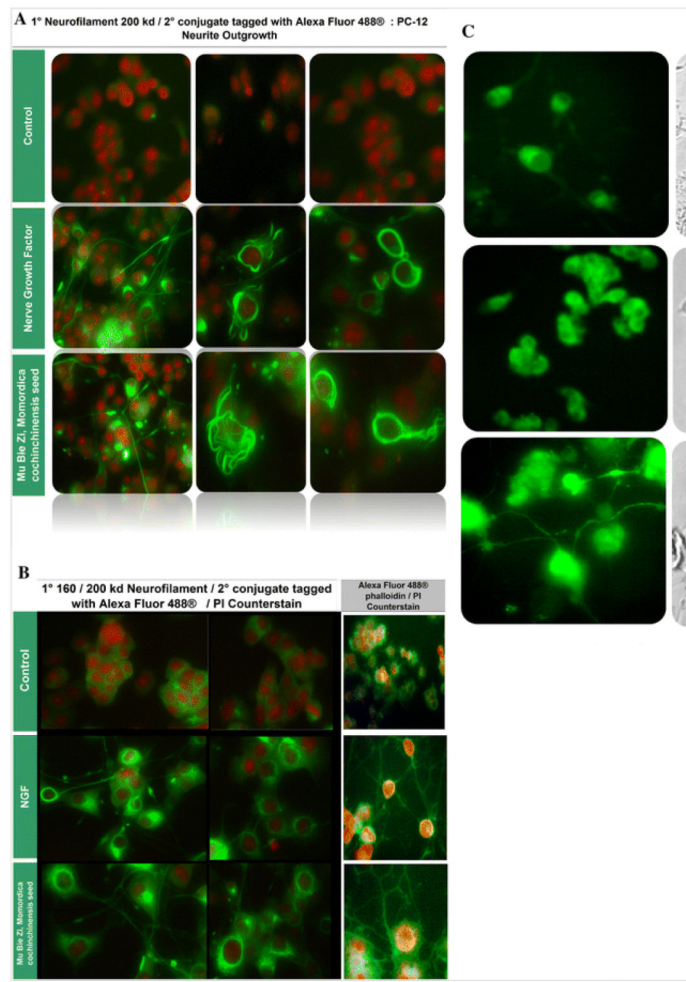


Fig. 3.

A Changes in NF-200 in PC12 cells at 7 days controls; controls (*top*) NGF 0.5 µg/mL (*mid*) and MCS extract (150 µg/mL) (*bottom*). **B** Changes in NF-160/200 kD and filamentous F-Actin in PC12 cells at 7 days controls; controls (*top*) NGF 0.5 µg/mL (*mid*) and MCS extract (150 µg/mL) (*bottom*). **C** Changes in tubulin (*left*) and corresponding morphology (*right*)—in PC12 cells at 7 days controls; controls (*a*) NGF 0.5 µg/mL (*b*) and MCS extract (150 µg/mL) (*c*)

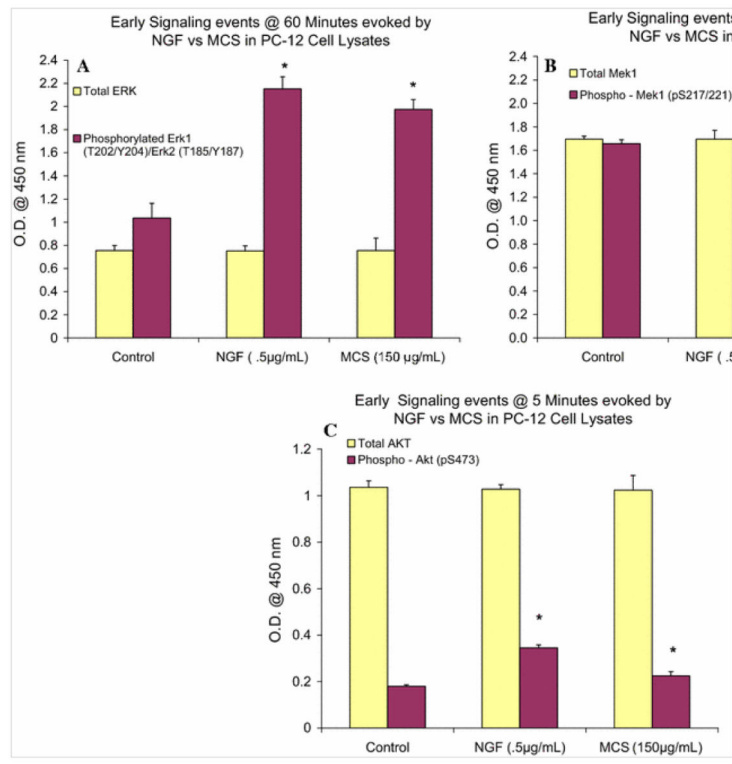


Fig. 4. **a** Early pERK1/2 signaling of NGF versus MCS exposure to PC12 Cells. The data represent relative Total ERK1/2 and pERK1/2 at 60 min. The data are expressed as the mean \pm SEM, $n = 4$. Significant differences from the control were evaluated using a one-way ANOVA, with a Tukey post hoc test, $*P < 0.05$. **b** Early MEK signaling of NGF versus MCS exposure to PC12 Cells. The data represent relative Total MEK and pMEK at 60 min. The data are expressed as the mean \pm SEM, $n = 4$. Significant differences from the control were evaluated using a one-way ANOVA, with a Tukey post hoc test, $*P < 0.05$. **c** Early AKT signaling of NGF versus MCS exposure to PC12 Cells. The data represent relative Total AKT and pAKT at 5 min. The data are expressed as the mean \pm SEM, $n = 4$. Significant differences from the control were evaluated using a one-way ANOVA, with a Tukey post hoc test, $*P < 0.05$

Table 1

Statistical and numerical data on neurite outgrowth parameters by image analysis

| Image analysis—MCS versus NGF | | | | |
|-----------------------------------|----------------|-------------------------------------|---|----------------|
| | [-] Control | [+] Control | <i>Mu Bie Zi, Momordica cochinchinensis</i> | |
| | No treatment | Nerve growth factor-7S 0.5 µg/mL | 4 µg/mL | 34 µg/mL |
| Total cell count/frame | 412.75 ± 70.72 | 208.78 ± 9.53 | 530.00 ± 71.18 | 342.00 ± 66.89 |
| Total neurite count/frame | 11.38 ± 2.52 | 81.00 ± 7.19 | 8.83 ± 1.83 | 23.60 ± 8.79 |
| Total neurite length (µm)/frame | 26.08 ± 5.29 | 1117.67 ± 107.47 | 36.45 ± 9.85 | 224.68 ± 88.56 |
| Average neurite length (µm)/frame | 2.20 ± 0.10 | 14.41 ± 0.94 | 4.32 ± 1.20 | 10.77 ± 1.87 |
| Neurite count/cell | 0.01 ± 0.01 | 0.40 ± 0.04 | 0.02 ± 0.01 | 0.08 ± 0.03 |
| Neurite length (µm)/cell | 0.07 ± 0.02 | 5.52 ± 0.62 | 0.09 ± 0.03 | 0.79 ± 0.31 |
| Min. neurite length (µm) | 1.29 ± 0.12 | 3.14 ± 0.43 | 1.42 ± 0.23 | 2.76 ± 0.55 |
| Max. neurite length (µm) | 3.58 ± 0.42 | 41.93 ± 3.11 | 7.77 ± 0.32 | 27.79 ± 1.09 |